Comparative study of the effect of resonances of the weakly bound nuclei ^{6,7}Li on total fusion with light to heavy mass targets

A. Gómez Camacho,[1,*] A. Diaz-Torres,[2] and H. Q. Zhang[3,4]

[1]*Departamento del Acelerador, Instituto Nacional de Investigaciones Nucleares, Apartado Postal 18-1027, Codigo Postal 11801, Distrito Federal, Mexico*

[2]*Department of Physics, University of Surrey, Guildford, GU2 7XH, United Kingdom*

[3]*China Institute of Atomic Energy, Beijing 102413, China*

[4]*Department of Technical Physics, Beijing University 100871 Beijing, China*

(Received 28 January 2019; published 15 May 2019)

A systematic study of total fusion involving the weakly bound nuclei ^{6,7}Li with several light to heavy mass targets at Coulomb energies is presented. Emphasis is given to the role of resonance states ($l = 2, J^{\pi} = 3^{+}, 2^{+}, 1^{+}$ of ^{6}Li and $l = 3,\ J^{\pi} = 7/2^{-}, 5/2^{-}$ of ^{7}Li) on the total fusion excitation function. A comparative analysis of the effects of resonant breakup on total fusion is performed for both projectiles, using the continuum-discretized coupled-channel (CDCC) framework. The calculations demonstrate that (i) resonant breakup couplings play a more important role in total fusion than nonresonant couplings, (ii) resonance states with short half-lives are very important for total fusion, as incident energies decrease toward the Coulomb barrier energy where incomplete fusion dominates, and (iii) resonance states with long half-life act as quasibound inelastic states, playing a crucial role in complete fusion.

DOI: 10.1103/PhysRevC.99.054615

I. INTRODUCTION

Reaction mechanisms in collisions of weakly bound projectiles with stable targets have been intensively investigated in the last decade [1–7]. In particular, fusion and breakup reactions induced by these projectiles have been studied both theoretically and experimentally. Among the most studied weakly bound projectiles are stable ^{6,7}Li and ^{9}Be, and unstable ^{6,8}He, ^{7,11}Be, ^{8}B, and ^{17}F nuclei, in collisions with diverse stable targets, ranging from ^{7}Li to ^{238}U. In these studies, the effects of breakup of the projectile on other reaction channels, such as elastic scattering and fusion, have received close attention, as these effects can be very pronounced. Since the intensities of weakly bound stable beams are several orders of magnitude larger than those presently available for exotic beams, measurements with stable weakly bound nuclei have dominated the experimental studies. Most experiments determine fusion and elastic scattering cross sections because direct measurements of breakup yields are very difficult to carry out. However, by using coincidence techniques, exclusive breakup yields have been measured for the system ^{6}Li + ^{59}Co [8,9], not only for elastic breakup but also for sequential breakup from several transferand/or pickup mechanisms.

The breakup of projectiles with low binding energies produces strong effects on fusion, leading to specific fusion processes. For instance, complete fusion (CF) occurs when the whole projectile is captured by the target. However, CF can be direct when fusion takes place without a previous breakup, or sequential when all projectile fragments are captured after breakup. When some fragments are captured while others escape, the process is called incomplete fusion (ICF). Total fusion (TF) refers to the sum of CF and ICF. Noncapture breakup (NCBU) happens when none of the breakup fragments is captured by the target nucleus. Certainly, a realistic evaluation of the effect of breakup on fusion must take into account couplings to all of the collective degrees of freedom involved in the reaction. For instance, NCBU can be elastic, in which the fragments interact elastically with the target, or it can be inelastic. In this case, inelastic excitations of the target and/or projectile (prior to breakup) are produced. All of these processes are schematically represented in Ref. [10], in which the ICF cross section is interpreted as a part of the inclusive, nonelastic breakup cross section.

The effect of breakup (direct and sequential) on complete and total fusion has been strongly debated in recent years [8,9,11–14]. It has been established that CF for several weakly bound nuclei in reactions with heavy targets becomes suppressed at energies above the Coulomb barrier. This suppression has been widely associated with the low threshold energies for breakup, resulting in the loss of flux of intact nuclei at the Coulomb barrier radius, as breakup of the projectile occurs at distances beyond the radius of the Coulomb barrier. However, at sub-barrier energies, reaction mechanisms involving weakly bound nuclei may be more complex. This is because breakup of short-lived projectile-like nuclei (after transfer of nucleons) is also an important process that may predominate over the direct breakup of incident projectiles, whereby CF becomes enhanced [15–18]. For example, for the two-body nuclei ^{6}Li (α-d) and ^{7}Li (α-t), recent measurements [15]

*arturo.gomez@inin.gob.mx

have established that significant breakup of ^{6}Li is triggered by either neutron transfer to targets, leading to sequential p-α breakup of the projectile-like nucleus ^{5}Li, or d pickup by ^{6}Li, leading to sequential breakup of $^{8}\mathrm{Be} \rightarrow \alpha + \alpha$. For ^{7}Li, important breakup intensities have been observed for p pickup, leading to $\alpha + \alpha$ coincidences, and $2n$ stripping, leading to sequential $p + \alpha$ breakup. Direct breakup of ^{6,7}Li also has a significant effect on fusion at low energies, mainly by its contribution to ICF. Since ICF becomes increasingly relevant with decreasing incident energies, the direct breakup process inhibits CF.

The continuum-discretized coupled-channel (CDCC) method [11–14,19–21] is commonly used to quantify the impact of continuum breakup states on reaction observables. In this approach, the continuum wave functions describing the projectile breakup are grouped in bins that can be treated as usual bound inelastic states, as they are described by square-integrable wave functions. The effects of continuum couplings on other reaction processes, such as elastic scattering and fusion, have been studied for many heavy-ion systems; for instance, fusion of ^{6,7}Li with ^{59}Co and ^{209}Bi [22] targets and fusion of ^{11}Be with ^{208}Pb [23]. In reactions of the halo ^{11}Be with ^{209}Bi, total fusion has been calculated by the absorption of the center of mass of ^{11}Be. Since breakup occurs mainly by $^{11}\mathrm{Be} \rightarrow {}^{10}\mathrm{Be} + n$, thus capture of the center of mass of ^{11}Be implies the absorption of ^{10}Be, which carries most of the mass and charge of ^{11}Be. However, this is not the case for nuclei such as ^{6,7}Li, for which the main direct breakup channels are $^{6}\mathrm{Li} \rightarrow \alpha + d$ and $^{7}\mathrm{Li} \rightarrow \alpha + t$. In both cases, the fragment masses are not so different, thus fusion cannot be calculated by the absorption of the center of mass of ^{6,7}Li. For this reason, two short-range absorption potentials were used to account for capture of α and d for ^{6}Li or α and t for ^{7}Li [22]. In this way, the calculated total fusion includes CF (both direct and sequential) when both fragments are inside the region of the two absorptive fusion potentials. Similarly, ICF is accounted for when only one fragment is in the respective fusion absorption region while the other fragment is outside and survives the capture process. Although, in the CDCC model, couplings from the elastic channel to breakup and inelastic states of reaction partners can be included [24], it has a serious drawback because an explicit separation of CF and ICF is not possible without ambiguity, and only TF can be calculated unambiguously [25]. Recently, some efforts have been made for the simultaneous calculation with CDCC of CF and ICF [26], for ^{6,7}Li with ^{209}Bi and ^{198}Pt targets [26] and ^{6}Li with ^{144,154}Sm targets [27]. Notwithstanding, some ambiguity still remains as to whether the absorption of a given fragment comes from the CF or ICF process. More transparent calculations, within classical [28,29] and quantum mechanical [30] methods, have been proposed to unambiguously separate CF and ICF. For instance, the classical dynamical reaction model was described in Refs. [28,29] and implemented in the PLATYPUS code [31]. This model unambiguously determines CF and ICF contributions to TF. The contributions to CF and ICF from sequential and direct breakup processes are explicitly calculated [32]. However, this classical model cannot treat sub-barrier fusion determined by quantum tunneling.

The effect of breakup of weakly bound nuclei on elastic scattering has also been a subject of intense research in recent years. Among the most studied cases are elastic scattering of ^{6,7}Li projectiles with targets of diverse masses. ^{6,7}Li have resonance states: $l = 2, J^{\pi} = 3^{+}, 2^{+}, 1^{+}$ for ^{6}Li and $l = 3, J^{\pi} = (7/2)^{-}, (5/2)^{-}$ for ^{7}Li. Resonance states, due to their definite half-life, may have particular effects on both elastic scattering and fusion. For instance, the effect on elastic scattering from resonance and nonresonance continuum states of ^{6}Li with targets ^{28}Si, ^{58}Ni, and ^{144}Sm have been presented in Refs. [33,34]. The CDCC calculations show that couplings among continuum resonance states of ^{6}Li produce stronger repulsive polarization potentials than those for nonresonance states. It was found that couplings to resonance states produce strong incident flux absorption, particularly at backward angles and for energies around the barrier. On the other hand, the study of the effect on TF from resonance and nonresonance couplings, for the same projectile ^{6}Li on targets ^{28}Si, ^{59}Co, ^{96}Zr, ^{198}Pt, ^{209}Bi, and ^{144,154}Sm was reported in Refs. [27]. It was found that couplings to resonance states produce strong repulsive polarization potentials. Hence, fusion becomes suppressed by these states. Couplings to nonresonance breakup states yield slightly repulsive potentials at energies well above the Coulomb barrier. However, for heavy targets and for energies around the barrier, the polarization potentials become attractive, enhancing fusion.

Certainly, due to the different decay half-lives, resonance states may have different effects on fusion. For instance, since the collision time is of the order of 10^{-21} s, the 3^{+} resonance state of ^{6}Li, having a half-life of about $\tau \approx 2.74 \times 10^{-20}$ s, may behave as a quasibound inelastic state when approaching the target and even break up during the outgoing branch of its trajectory. Thus, this state would contribute to CF but not to ICF. The other resonance states 2^{+} and 1^{+}, having shorter half-lives, $\approx 3.8 \times 10^{-22}$ and $\approx 1.56 \times 10^{-22}$ s, respectively, may breakup when approaching the target and contribute to ICF and NCBU processes. On the other side, the prompt breakup of nonresonance states could have a more significant effect on ICF. As for the nucleus ^{7}Li, which shows resonance states $l = 3$, $7/2^{-}$ and $5/2^{-}$ with half-lives 7.08×10^{-21} and 0.75×10^{-21} s, respectively, may contribute mostly to ICF. These processes are schematically represented in Fig. 1. These breakup processes may be particularly important at energies close to and below the barrier. At higher energies, it is expected that the effects on fusion of resonance and nonresonance states would become similar and contribute mainly to CF.

The experimental measurements and CDCC calculations of Santra *et al.* of $^{6}\mathrm{Li} \rightarrow \alpha + d$, in reaction with ^{209}Bi [35], show that breakup into $\alpha + d$ occurs mainly by the excitation of the 3^{+} resonance. Hence, this resonance may have important effects on fusion. However, nucleon transfer followed by breakup processes of projectile-like nuclei (transfer triggered breakup) have important yields. Recent calculations based on the classical dynamical model with stochastic breakup [32] address the impact of prompt and delayed breakup of ^{6}Li on ICF, showing that the contribution to ICF from excitation of the 3^{+} resonance is negligible. These results are explained in terms of the long half-life of this resonance compared to the 2^{+} and 1^{+} ones.

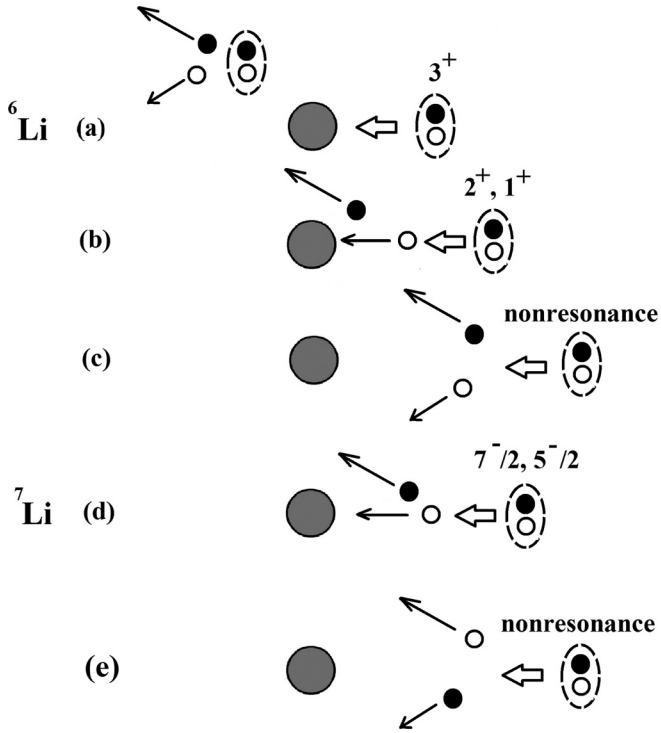

FIG. 1. Some reaction pathways involving resonance and nonresonance states of the weakly bound nuclei ^{6}Li [(a)–(c)] and ^{7}Li [(d) and (e)]. The effects on CF and ICF depend on the half-lives of these states.

In the present work, we discuss comparative and systematic CDCC calculations on the effect on TF, of couplings to resonance states of the weakly bound nuclei ^{6,7}Li, in collisions with ^{27}Al, ^{28}Si, ^{59}Co, ^{144}Sm, ^{198}Pt, and ^{209}Bi targets. The main purpose is to understand the role of resonance states of the projectiles in the dynamics of prompt and delayed (direct) breakup, and how these states affect TF at energies around the Coulomb barrier. In the calculations of TF, and to determine the effect of a given resonance or a group of them, couplings to these states are omitted from the full discretized CDCC breakup space. So, by comparing these results with those with the full space, the effects can be obtained. On the same footing, corresponding effects from nonresonance states can be calculated by considering only couplings within the resonance subspace. In the calculations, the main breakup (direct) channels for ^{6,7}Li are assumed to be α-d and α-t, respectively. TF is determined using two short-range, imaginary fusion potentials for the interactions between the fragments and the targets [22].

The paper is organized as follows. Section II presents the results of the calculations of TF and the effects of resonance and nonresonance states. Also, the particular effects of long as well as short-lived resonances on TF are discussed. Finally, a summary is given in Sec. III.

II. TOTAL FUSION AND EFFECTS OF RESONANCE AND NONRESONANCE STATES

A complete description of the CDCC formalism is given in Refs. [19–21]. Also, a formal description of how the CDCC is used to study the effects of resonance states on elastic scattering is presented in Refs. [33,34]. The coupled-channel equations for any radial wave function $\psi_\beta^P(\mathbf{r})$ of the projectile in the excited state β and the target in its ground state Φ_0^T are

$$\left[\hat{T}_{R,K} + U^{(J)}_{\beta,\beta}(R) - (E - \epsilon_0 - \varepsilon_\beta)\right]F^{(J)}_\beta(R) = -\sum_{\beta' \neq \beta}\left[U^{(J)}_{\beta,\beta'}(R)\right]F^{(J)}_{\beta'}(R). \quad (1)$$

In this equation, J and E are the total angular momentum and collision energy, respectively. ϵ_0 represents the energy of the ground state of the target, while ε_β is the energy of the ground or any discrete breakup state β of the projectile. $U^{(J)}_{\beta,\beta'}$ are the diagonal ($\beta = \beta'$) and nondiagonal ($\beta \neq \beta'$) coupling matrix elements given by

$$U^{(J)}_{\beta\beta'}(R) = \langle u_\beta | \hat{V}_{d(t)T}(\mathbf{r}_{d(t)T}) + \hat{V}_{\alpha T}(\mathbf{r}_{\alpha T}) | u_{\beta'} \rangle, \quad (2)$$

where $u_\beta(\mathbf{r})$ are the normalized square-integrable wave functions known as bin states [19,33,34]. Integrations in Eq. (2) are performed over the relative vectors $\mathbf{r}$, so that the matrix elements only depend on the separation R between the target and the projectile. For ^{6}Li, these vectors are related by $\mathbf{r}_{\alpha T} = \mathbf{R} + \frac{4}{6}\mathbf{r}$ and $\mathbf{r}_{dT} = \mathbf{R} - \frac{2}{6}\mathbf{r}$, while for ^{7}Li, $\mathbf{r}_{\alpha T} = \mathbf{R} + \frac{4}{7}\mathbf{r}$ and $\mathbf{r}_{tT} = \mathbf{R} - \frac{3}{7}\mathbf{r}$. Equations (1) are solved numerically with the usual scattering boundary conditions using the FRESCO code described in Ref. [36]. Total fusion cross section $\sigma_{\rm TF}$ is determined by the inclusion of two short-range imaginary potentials $W(r_{d(t)T})$ and $W(r_{\alpha T})$ for the absorptions between the fragments with the target. That is, $\sigma_{\rm TF} = \sum_J \sigma^{(J)}_{\rm TF}$, where the partial cross section reads,

$$\sigma^{(J)}_{\rm TF} = \frac{2}{\hbar v}\sum_\beta \left\langle F^{(J)}_\beta(R) \middle| W(r_{d(t)T}) + W(r_{\alpha T}) \middle| F^{(J)}_\beta(R) \right\rangle, \quad (3)$$

where v is the incident relative projectile-target velocity. For ^{6}Li, the relative vectors are given by $\mathbf{r}_{\alpha T} = \mathbf{R} + \frac{4}{6}\mathbf{r}$ and $\mathbf{r}_{dT} = \mathbf{R} - \frac{2}{6}\mathbf{r}$, while for ^{7}Li, $\mathbf{r}_{\alpha T} = \mathbf{R} + \frac{4}{7}\mathbf{r}$ and $\mathbf{r}_{tT} = \mathbf{R} - \frac{3}{7}\mathbf{r}$.

In this section, we describe the calculations of total fusion cross sections for reactions between the projectile ^{7}Li with targets ^{27}Al, ^{59}Co, ^{144}Sm, and ^{209}Bi for incident energies around the corresponding Coulomb barriers. Converged CDCC calculations of total fusion for the ^{6}Li projectile with targets ^{28}Si, ^{59}Co, ^{96}Zr, ^{198}Pt, and ^{209}Bi have been reported in Ref. [37]. A comparative study on the effects of resonances $7/2^-$ and $5/2^-$ of ^{7}Li on fusion is presented, with respect to those produced by resonance states, 3^+, 2^+, and 1^+ of ^{6}Li.

A. Model space and potentials

For the reactions with ^{7}Li, the same discretization procedure as in Ref. [37] is followed. The calculations of the ground $3/2^-$, $E_{\rm thres} = 2.47$ MeV, bound $1/2^-$, $E_{\rm thres} = 1.99$ MeV, and discretized breakup state wave functions of $^7\text{Li} \rightarrow \alpha + t$, are constructed by using the α-t interaction of Ref. [22]. For energies around the barrier, discrete breakup states are constructed (relative to the threshold energy $E_{\rm thres} = 2.47$ MeV) from an initial energy $\varepsilon_{\rm min} = 0$ MeV up to a maximum energy $\varepsilon_{\rm max} = 6.8$ MeV, where convergence is achieved. For energies well above the barrier, $\varepsilon_{\rm max} = 8.0$. The maximum

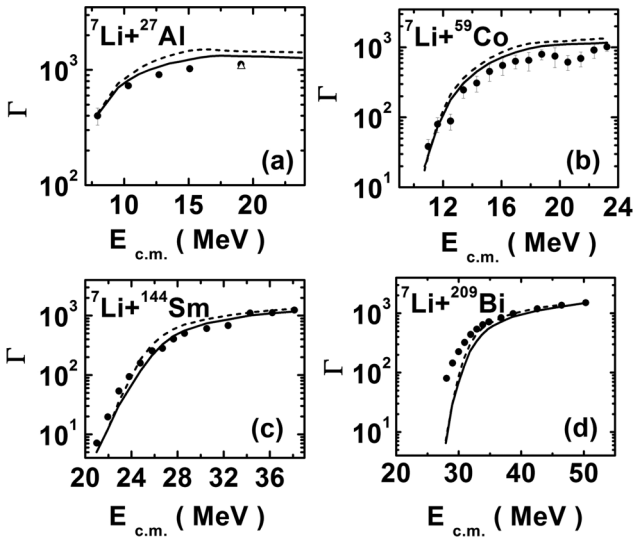

FIG. 2. Total fusion calculations (solid line) with the complete discretized breakup space for ^{7}Li with targets ^{27}Al, ^{59}Co, ^{144}Sm, and ^{209}Bi. The data shown are from Refs. [42,43] for ^{27}Al, [44] for ^{59}Co, [45,46] for ^{144}Sm, and [47] for ^{209}Bi. The dashed lines show the elastic channel calculations without couplings to continuum breakup states.

relative angular momentum between the fragments α and t is set to $l = 3$. Higher values do not have an effect on the convergent calculations. Bin widths are conveniently modified in the presence of resonance states $l = 3, J^\pi = 7/2^-, 5/2^-$. Finer discretization steps $\Delta\epsilon$ [22] should be assumed in order to avoid double counting and to obtain centroid resonance energies and widths close to the experimental values, $\varepsilon_{7/2^-} = 2.16$ MeV, $\Gamma_{7/2^-} = 0.093$ MeV, $\varepsilon_{5/2^-} = 4.21$ MeV, and $\Gamma_{5/2^-} = 0.88$ MeV.

As in the case of ^{6}Li [37], two short-range absorption potentials $W_{\alpha T}$ and W_{tT} are used for the interactions between the fragments α and t with the target T. The parameters of these volume Woods-Saxon potentials are the same for both fragments and for all the targets. These are set to $W_0 = -50$ MeV, diffuseness $a_0 = 0.1$ fm, and reduced radius $r_0 = 0.8$ fm. The potentials $\hat{V}_{\alpha T}$ and $\hat{V}_{tT}$ of Eq. (2), include Coulomb and nuclear parts. As for the nuclear part, the free-parameter double-folding São Paulo potential (SPP) [38,39] is used for the interaction between the α particle and target, while the Winther potential [40] for tritium and target.

B. Results

The results of CDCC calculations for total fusion cross sections for ^{7}Li with targets ^{27}Al, ^{59}Co, ^{144}Sm, and ^{209}Bi are shown in Fig. 2. The TF calculations (solid lines) of Figs. 2(a)–2(d) show that couplings to continuum breakup states of the projectile suppress fusion compared to those calculations without couplings (dashed lines), particularly for energies above the barrier V_B. The elastic channel calculations, i.e., without couplings to continuum states, correspond to fusion through the elastic channel in which only the term $U^{(J)}_{0,0}(R)$ [$\beta = 0$ of Eq. (2)] is considered. In Fig. 2, it is also observed that as the collision energy approaches the barrier, the effect of breakup couplings becomes negligible. This behavior differs from that for the ^{6}Li projectile, for which an appreciable effect is still present at energies below the barrier [37]. This fact can be due to the smaller breakup threshold of ^{6}Li (1.47 MeV), so that as the collision energy decreases, an appreciable breakup probability remains. The disagreement between the calculations for $\sigma_{\rm TF}$ with the data, as observed for ^{27}Al, ^{59}Co at the higher energies, and ^{144}Sm, and ^{209}Bi at the lowest energies may be due to two factors: (a) the use of global projectile-target nuclear interactions and (b) the effect of sequential, transfer triggered breakup mechanisms, as well as, couplings to excited states of the target. Couplings to the latter states are not considered in the present calculations. For instance, for ^{7}Li + ^{209}Bi, it was suggested in Ref. [22] that the triton-transfer channel may be very important for explaining the experimental total fusion cross sections at energies around the Coulomb barrier. Very recent measurements [41] have confirmed the importance of this channel for the yield of specific incomplete fusion products. In fact, the impact of this channel on the CF cross sections can be quantified with the novel approach suggested in Ref. [10].

To determine the effects on fusion of resonance states $l = 2, J^\pi = 3^+, 2^+, 1^+$ of ^{6}Li and $l = 3, J^\pi = 7/2^-, 5/2^-$ of ^{7}Li, the same procedure is followed as in Ref. [37]. That is, the effect of a given resonance (or group of resonances), is calculated by omitting all bin states of that resonance (resonances) from the full discretized breakup space. This is equivalent to disregarding the couplings to these states in Eq. (3). The effect is given in terms of Γ_i defined by

$$\Gamma_i = 1 - \frac{\sigma_{\rm TF}}{\sigma_i}, \tag{4}$$

where $\sigma_{\rm TF}$ is total fusion with all couplings in the full breakup space included. σ_i, $i = R$ is the fusion calculation when resonance ($i = R$) states are considered but nonresonance states are omitted. The opposite case is given by σ_i, $i = {\rm NR}$, which is the fusion calculation when resonance states are omitted. σ_i, $i = {\rm el}$, corresponds to fusion through the elastic incident channel without couplings to continuum breakup states of the projectile.

The long-dashed, dashed-dotted, and short-dashed lines in Figs. 3(a)–3(d) show the results of $\Gamma_{\rm R}$, $\Gamma_{\rm NR}$ and $\Gamma_{\rm el}$ for ^{7}Li with targets ^{27}Al, ^{59}Co, ^{144}Sm, and ^{209}Bi. Similar calculations for the projectile ^{6}Li with targets ^{28}Si, ^{59}Co, ^{96}Zr, ^{198}Pt, and ^{209}Bi have been reported in Ref. [37]. To facilitate comparison between the two projectiles, we reproduce these results in Figs. 4(a)–4(e). The dashed lines show the results when couplings to resonance states $3^+, 2^+, 1^+$ are considered while the dashed-dotted lines correspond to nonresonance states.

It is observed in Figs. 3 and 4 that the effect of continuum couplings on total fusion is stronger for ^{6}Li than for ^{7}Li, for all targets. For instance, for ^{6}Li with the target ^{28}Si, $\Gamma_{\rm el}$ increases as the energy approaches the barrier, while for ^{7}Li + ^{27}Al, $\Gamma_{\rm el}$ rapidly approaches smaller values. For targets ^{59}Co and ^{209}Bi, $\Gamma_{\rm el}$ peaks at smaller values for ^{7}Li than for ^{6}Li. We also notice than the omission of couplings to resonance states, shown by the dashed-dotted lines, has a very strong effect on fusion. As a matter of fact, not only

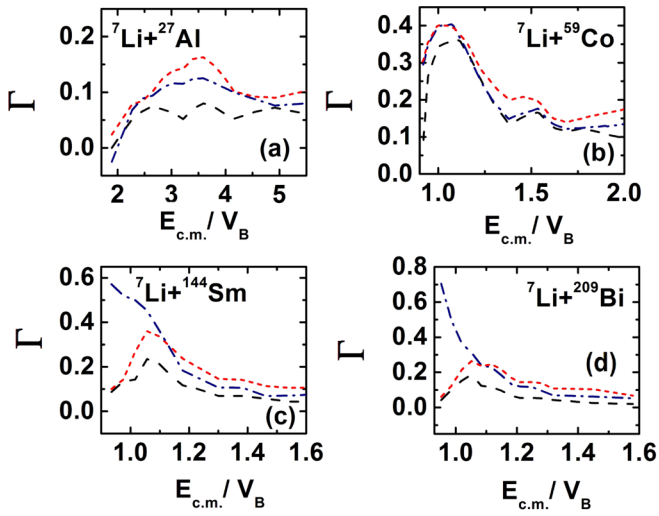

FIG. 3. Effects on fusion when resonance (long-dashed lines) and nonresonance (dashed-dotted lines) subspaces of ^{7}Li are considered in reaction with targets ^{27}Al, ^{59}Co, ^{144}Sm, and ^{209}Bi. The short-dashed lines correspond to the elastic channel.

Γ_{NR} reaches higher values for reactions with ^{6}Li than for ^{7}Li for similar targets, but also $\Gamma_{NR} > \Gamma_{el}$ for the heavier targets at low energies. This means that when couplings to resonance states of the projectiles are accounted for, they should produce a very strong fusion suppression. This finding is supported by the calculations in which nonresonance states

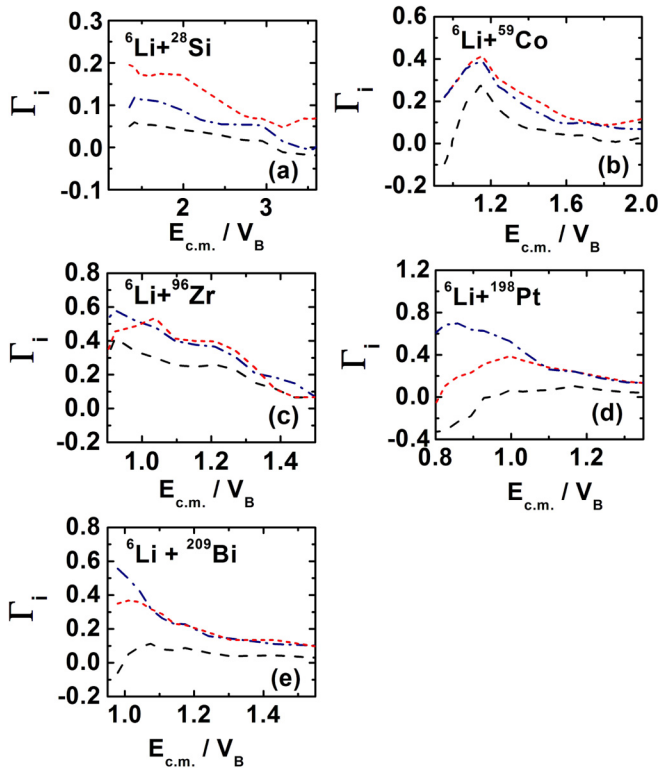

FIG. 4. Same as Fig. 2, but for ^{6}Li with targets ^{28}Si, ^{59}Co, ^{96}Zr, ^{198}Pt, and ^{209}Bi.

are omitted, i.e., Γ_R (long-dashed lines) has smaller values than Γ_{NR} (dashed-dotted lines) in all cases. That is, fusion through resonance states is more significant than through nonresonance ones. Also, it is observed that for high energies Γ_R and Γ_{NR} approach similar decreasing values. The energy dependence of Γ_R and Γ_{NR} of Figs. 3 and 4 can be understood in terms of the prompt breakup of nonresonance states and the delayed breakup of resonance ones. Nonresonance states breakup as soon as the projectile interacts with the target, mainly by Coulomb excitation. At low collision energies, close to the barrier, these states may have a more significant contribution to ICF and NCBU processes. At very high energies, well above the barrier, resonance and nonresonance states contribute mainly to CF. In this situation, the projectile is captured by the target without a previous breakup. This explains why Γ_R and Γ_{NR} approach to a similar decreasing behavior. On the other hand, resonance states can play a very peculiar role on fusion at collision energies around the barrier. Those resonance states with shorter half-lives may breakup when approaching the target and contribute mostly to ICF than to CF. On the contrary, those resonance states with longer half-lives can have a more important effect on CF and even may breakup (from a time-dependent classical viewpoint [32]) during the outgoing branch of the projectile-target trajectory. In this interpretation, long-lived resonance states do not have any effect on fusion.

In the next calculations, we try to disentangle the particular effects on fusion produced by a single resonance state of the projectiles ^{6,7}Li. We study these effects by omitting couplings to that resonance state from the full discretized energy space. For instance, for the case of ^{6}Li, the dashed-dotted lines of Figs. 5(a)–5(e) correspond to Γ_i, $i = 3^+$, that is, couplings to the resonance states 2^+, 1^+ are not allowed, but those from the 3^+ are considered. Similarly, the dashed lines show the contrary effect, Γ_i, $j = 2^+, 1^+$ [see Eq. (4)], where couplings to the resonance 3^+ are omitted, while those from 2^+ and 1^+ are included. It is observed that as the target mass increases and for energies well above the barrier, Γ_{3^+} and $\Gamma_{2^+,1^+}$ approach similar decreasing behaviors. However, as the energy decreases toward the barrier, $\Gamma_{2^+,1^+}$ becomes progressively smaller than Γ_{3^+}. This shows that, the effects of couplings to resonance states 2^+ and 1^+ become more significant because fusion is strongly suppressed by these resonances. As pictured in Figs. 1(a)–1(e), this behavior can be interpreted as follows: (a) Since the half-life of resonance 3^+ ($\tau \approx 2.74 \times 10^{-20}$ s) is one order of magnitude longer than the typical collision time 10^{-21} s, this state behaves as a quasibound inelastic excited state and thus may contribute more to CF than to ICF. Also, the projectile in this state may breakup during the outgoing branch of its trajectory in which case it does not have any effect on fusion. Couplings to this state produce a net attractive polarization potential that lowers the barrier and hence enhances fusion. (b) Resonance states 2^+ and 1^+, which have shorter half-lives ($\approx 3.8 \times 10^{-22}$ and $\approx 1.56 \times 10^{-22}$ s respectively) than the typical collision time, may break up during the incoming part of the trajectory and contribute mostly to ICF. Couplings to these resonance states produce repulsive polarization potentials that suppress fusion. It is important to point out that total fusion is dominated

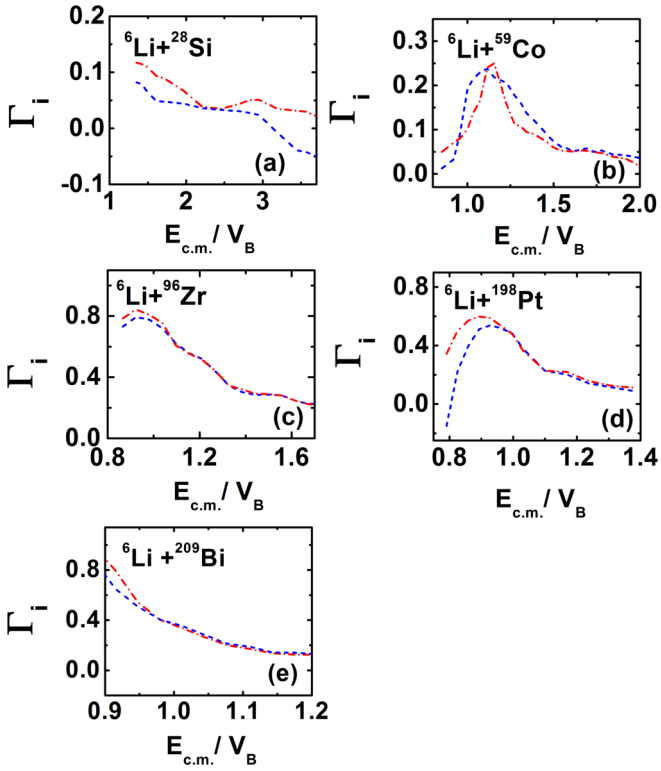

FIG. 5. Effects on fusion for ^{6}Li. The dashed-dotted lines represent the effect when the resonance 3^+ is included in the discretized breakup space but 2^+, 1^+ are excluded. The dashed lines represent the opposite effect.

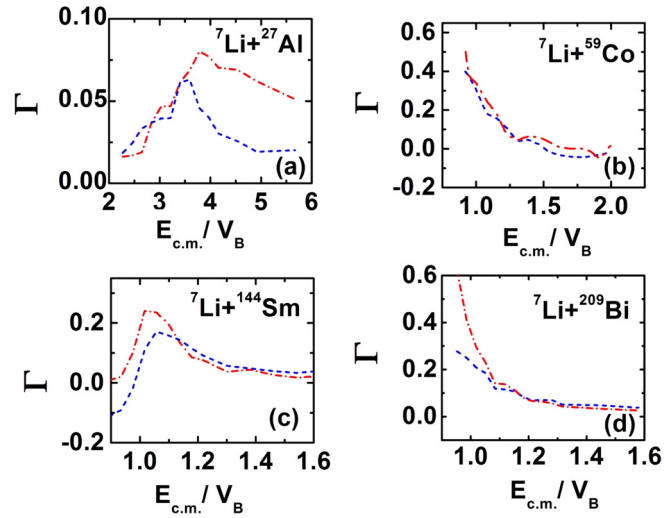

FIG. 6. Effects on fusion when resonances $5/2^-$ (dashed lines) and $7/2^-$ (dashed-dotted lines) of ^{7}Li with targets ^{27}Al, ^{59}Co, ^{144}Sm, and ^{209}Bi.

by incomplete fusion at very low energies for many nuclear systems involving weakly bound projectiles. For instance, for $^{6}\mathrm{Li} + {}^{144}\mathrm{Sm}$, ICF is several orders of magnitude more significant than CF at energies of around 5 MeV below the barrier [48]. This fact is in accordance with our calculations because fusion through resonances 2^+ and 1^+ approaches TF, σ_{TF}, at energies below the barrier, where ICF becomes more significant. (c) Nonresonance states break up promptly and mostly feed noncapture breakup.

As for the projectile ^{7}Li, this nucleus shows resonances $l = 3$, $7/2^-$ and $5/2^-$ [represented in Fig. 1(d)] with widths 0.093 and 0.88 MeV respectively. The half-lives of these states are 7.08×10^{-21} and 0.75×10^{-21} s, which are of the order of magnitude as the collision time. These states, once excited, may contribute mostly to ICF at low energies. In fact, it would be expected that the resonance state $5/2^-$, having a slightly shorter half-life, would break up sooner and play a more important role on ICF than the $7/2^-$. In Figs. 6(a)–6(d), we show the results of fusion when couplings to either resonance $5/2^-$ or $7/2^-$ are omitted from the complete discretized breakup space.

At high energies both effects tend to be similar and decreasing for all targets, that is, resonance states contribute mainly to CF. However, as the energy approaches the barrier, we observe that $\Gamma_{5/2^-}$ ($7/2^-$ omitted) diminishes more rapidly than $\Gamma_{7/2^-}$ ($5/2^-$ omitted) for the heavier targets. This means that fusion is more strongly suppressed by this resonance. At even lower energies as those shown in Figs. 5(b) and 5(d), it is expected that $\Gamma_{5/2^-}$ and $\Gamma_{7/2^-}$ approach lower values. Performing CDCC calculations at even smaller energies produces computational instabilities and were not carried out. So, at energies around and below the barrier, where total fusion starts being dominated by ICF, both resonance states $5/2^-$ and $7/2^-$ contribute mostly to it. Notwithstanding, the significance of the state $5/2^-$ becomes more important as the target mass increases.

III. SUMMARY

CDCC calculations of total fusion cross sections have been presented for the weakly bound ^{6,7}Li projectiles with a diversity of stable targets. The effect of resonance and nonresonance breakup states of these projectiles on total fusion has been studied by omitting couplings to those breakup subspaces from the complete discretized breakup space for ^{6,7}Li.

For ^{7}Li, it has been found that (1) total fusion through resonances $5/2^-$ and $7/2^-$ produces a more pronounced fusion yield than from nonresonance states. This finding is strongly related to the half-lives of the resonances. It was also determined that these resonances have a very important role in the incomplete fusion process at energies around the barrier. (2) The $5/2^-$ resonance state, having a shorter half-life, has a more significant effect on incomplete fusion at low energies than the $7/2^-$.

For ^{6}Li, with a long-lived 3^+ and two short-lived 2^+ and 1^+ resonance states, it was found that (1) the 3^+ state behaves as a bound quasi-inelastic state. Therefore, this resonance has more relevance on complete fusion than on incomplete fusion processes. (2) For the 2^+ and 1^+ states with half-lives smaller than the typical collision time ($\approx 10^{-21}$ s), breakup occurs during the incident part of the projectile-target trajectory, and thus they have a more significant effect on the incomplete fusion process at low energies.

ACKNOWLEDGMENTS

We appreciate the comments, suggestions, and discussions offered by Dr. Shan-Gui Zhou during the visit of Dr. A. Gómez to the Institute of Theoretical Physics of the Academy of Sciences, Beijing, China. Financial support is acknowledged by A.G. from CONACYT, México; H.Q.Z. from NSF China Grant No.11375266, and A.D.-T. from the STFC Grant No. ST/P005314/1.

[1] L. F. Canto, P. R. S. Gomes, R. Donangelo, and M. S. Hussein, Phys. Rep. **424**, 1 (2006).
[2] J. F. Liang and C. Signorini, Int. J. Mod. Phys. E **14**, 1121 (2005).
[3] N. Keeley, R. Raabe, N. Alamanos, and J. L. Sida, Prog. Part. Nucl. Phys. **59**, 579 (2007).
[4] N. Keeley, N. Alamanos, K. W. Kemper, and K. Rusek, Prog. Part. Nucl. Phys. **63**, 396 (2009).
[5] K. Hagino and N. Takigawa, Prog. Theor. Phys. **128**, 1061 (2012).
[6] B. B. Back, H. Esbensen, C. L. Jiang, and K. E. Rehm, Rev. Mod. Phys. **86**, 317 (2014).
[7] L. F. Canto, P. R. S. Gomes, R. Donangelo, J. Lubian, and M. S. Hussein, Phys. Rep. **596**, 1 (2015).
[8] F. A. Souza, C. Beck, N. Carlin, N. Keeley, R. Liguori Neto, M. M. de Moura, M. G. Munhoz, M. G. Del Santo, A. A. P. Suaide, E. M. Szanto, and A. Szanto de Toledo, Nucl. Phys. A **821**, 36 (2009).
[9] F. A. Souza, N. Carlin, C. Beck, N. Keeley, A. Diaz-Torres, R. Liguori Neto, C. Siqueira-Mello, M. M. de Moura, M. G. Munhoz, R. A. N. Oliveira, M. G. Del Santo, A. A. P. Suaide, E. M. Szanto, and A. Szanto de Toledo, Eur. Phys. J. A **44**, 181 (2010).
[10] J. Lei and A. M. Moro, Phys. Rev. Lett. **122**, 042503 (2019).
[11] K. Hagino, A. Vitturi, C. H. Dasso, and S. M. Lenzi, Phys. Rev. C **61**, 037602 (2000).
[12] C. Beck, N. Rowley, P. Papka, S. Courtin *et al.*, Nucl. Phys. A **834**, 440c (2010).
[13] C. Beck, N. Keeley, and A. Diaz-Torres, Phys. Rev. C **75**, 054605 (2007).
[14] P. F. F. Carnelli, D. Martinez Heimann, A. J. Pacheco *et al.*, Nucl. Phys. A **969**, 94 (2018).
[15] D. H. Luong *et al.*, Phys. Lett. B **695**, 105 (2011).
[16] D. H. Luong, M. Dasgupta, D. J. Hinde, R. du Rietz, R. Rafiei, C. J. Lin, M. Evers, and A. Diaz-Torres, Phys. Rev. C **88**, 034609 (2013).
[17] R. Rafiei, R. du Rietz, D. H. Luong, D. J. Hinde, M. Dasgupta, M. Evers, and A. Diaz-Torres, Phys. Rev. C **81**, 024601 (2010).
[18] A. Shrivastava *et al.*, Phys. Lett. B **633**, 463 (2006).
[19] Y. Sakuragi, M. Yahiro, and M. Kamimura, Prog. Theor. Phys. Suppl. **89**, 136 (1986).
[20] Y. Sakuragi, M. Yahiro, and M. Kamimura, Prog. Theor. Phys. **70**, 1047 (1983).
[21] N. Austern, Y. Iseri, M. Kamimura *et al.*, Phys. Rep. **154**, 125 (1987).
[22] A. Diaz-Torres, I. J. Thompson, and C. Beck, Phys. Rev. C **68**, 044607 (2003).
[23] A. Diaz-Torres and I. J. Thompson, Phys. Rev. C **65**, 024606 (2002).
[24] D. R. Otomar, J. Lubian, P. R. S. Gomes, and T. Correa, J. Phys. G: Nucl. Part. Phys. **40**, 125105 (2013).
[25] M. Boselli and A. Diaz-Torres, J. Phys. G: Nucl. Part. Phys. **41**, 094001 (2014).
[26] V. V. Parkar, V. Jha, and S. Kailas, Phys. Rev. C **94**, 024609 (2016).
[27] A. G. Camacho, J. Lubian, H. Q. Zhang *et al.*, Chin. Phys. C **41**, 124103 (2017).
[28] A. Diaz-Torres, D. J. Hinde, J. A. Tostevin, M. Dasgupta, and L. R. Gasques, Phys. Rev. Lett. **98**, 152701 (2007).
[29] A. Diaz-Torres, J. Phys. G: Nucl. Part. Phys. **37**, 075109 (2010).
[30] M. Boselli and A. Diaz-Torres, Phys. Rev. C **92**, 044610 (2015).
[31] A. Diaz-Torres, Comput. Phys. Commun. **182**, 1100 (2011).
[32] A. Diaz-Torres and D. Quraishi, Phys. Rev. C **97**, 024611 (2018).
[33] A. G. Camacho, A. Diaz-Torres, P. R. S. Gomes, and J. Lubian, Phys. Rev. C **91**, 014607 (2015).
[34] A. G. Camacho, A. Diaz-Torres, P. R. S. Gomes, and J. Lubian, Phys. Rev. C **93**, 024604 (2016).
[35] S. Santra, V. V. Parkar, K. Ramachandran, U. K. Pal, A. Shrivastava, B. J. Roy, B. K. Nayak, A. Chatterjee, R. K. Choudhury, and S. Kailas, Phy. Lett. B **677**, 139 (2009).
[36] I. J. Thompson, Comput. Phys. Rep. **7**, 167 (1988).
[37] A. G. Camacho, B. Wang, and H. Q. Zhang, Phys. Rev. C **97**, 054610 (2018).
[38] L. C. Chamon, D. Pereira, M. S. Hussein, M. A. Candido Ribeiro, and D. Galetti, Phys. Rev. Lett. **79**, 5218 (1997).
[39] L. C. Chamon, B. V. Carlson, L. R. Gasques *et al.*, Phys. Rev. C **66**, 014610 (2002).
[40] A. Winther, Nucl. Phys. A **594**, 203 (1995).
[41] K. J. Cook, E. C. Simpson, L. T. Bezzina, M. Dasgupta, D. J. Hinde, K. Banerjee, A. C. Berriman, and C. Sengupta, Phys. Rev. Lett. **122**, 102501 (2019).
[42] K. Kalita, S. Verma, R. Singh, J. J. Das, A. Jhingan, N. Madhavan, S. Nath, T. Varughese *et al.*, Phys. Rev. C **73**, 024609 (2006).
[43] I. Padron, P. R. S. Gomes, R. M. Anjos, J. Lubian, C. Muri *et al.*, Phys. Rev. C **66**, 044608 (2002).
[44] C. Beck *et al.*, Phys. Rev. C **67**, 054602 (2003).
[45] P. K. Rath, S. Santra, N. L. Singh, B. K. Nayak, K. Mahata, R. Palit, K. Ramachandran *et al.*, Phys. Rev. C **88**, 044617 (2013).
[46] P. K. Rath, S. Santra, N. L. Singh, B. K. Nayak, K. Mahata, R. Palit, and K. Ramachandran *et al.*, Nucl. Phys. A **874**, 14 (2012).
[47] M. Dasgupta, P. R. S. Gomes, D. J. Hinde, S. B. Moraes, R. M. Anjos, A. C. Berriman *et al.*, Phys. Rev. C **70**, 024606 (2004).
[48] P. K. Rath, S. Santra, K. Mahata, R. Tripathi, V. V. Parkar, R. Palit, B. K. Nayak, and N. L. Singh, in *Proceedings of the 62th DAE-BRNS Symposium on Nuclear Physics*, DAE Symposium on Nuclear Physics, Vol. 54 (2009), p. 310.